(Al)MCM-41 MOLECULAR SIEVES. ALUMINIUM DISTRIBUTION, UNIFORMITY AND STRUCTURE OF INNER SURFACE

Jiří DĚDEČEK[1], Naděžda ŽILKOVÁ[2], Josef KOTRLA[3] and Jiří ČEJKA[4,*]

J. Heyrovský Institute of Physical Chemistry, Academy of Sciences of the Czech Republic, Dolejškova 3, CZ-182 23 Prague 8, Czech Republic; e-mail: [1] jiri.dedecek@jh-inst.cas.cz, [2] zilkova@jh-inst.cas.cz, [3] kotrla@jh-inst.cas.cz, [4] cejka@jh-inst.cas.cz

Received May 27, 2003
Accepted August 18, 2003

The effect of the framework Al content and synthesis procedure on the number of framework Al atoms located on the surface of (Al)MCM-41 channels and the distribution of the Al atoms between single Al atoms and various Al-O-$(SiO)_{1,2}$-Al species was investigated. The total number of accessible framework Al atoms on the channel surface was obtained from the ion exchange capacity for Na^+ ions and pyridine adsorption. The number of Al pairs on the surface and their distribution between different local arrangements of the channel surface was estimated using VIS spectroscopy of Co^{2+} ions. At low framework Al contents, Al atoms occupy only accessible T sites on the surface of the channel walls. In aluminium-rich (Al)MCM-41, a significant part of Al atoms is incorporated inside the channel walls and these Al atoms do not form cationic sites. Al atoms on the wall surface preferentially form Al-O-$(SiO)_{1,2}$-Al sequences, enabling siting of divalent cations. Different synthesis procedures resulted in differences in Al distribution. The channel surface of the (Al)MCM-41 is formed by two regular local structures containing two types of deformed six-membered rings with Al-O-$(SiO)_{1,2}$-Al sequences forming cationic sites.

Keywords: Molecular sieves; (Al)MCM-41; Mesoporous materials; VIS spectroscopy; Local ordering; Cationic sites; Heterogeneous catalysis.

Mesoporous molecular sieves have recently attracted a great attention due to their potential for application in many areas of materials science[1–3]. Adsorption and particularly heterogeneous catalysis are expected to be the most promising fields for their application. Microporous molecular sieves exhibit catalytically desirable properties such as high surface area, tunable pore size, the possibility of tailoring the active sites and shape selectivity, but their utilisation is limited due to the pore dimensions not exceeding 0.8 nm. The discovery of mesoporous molecular sieves of the M41S family[4] opened extensive possibilities for preparation of new catalysts with uniform pores in the mesoporous range[5–7], easily accessible to bulky molecules and, thus, without limitations imposed by microporous materials.

doi:10.1135/cccc20031998

The introduction of trivalent elements (*e.g.* Al, Fe) into the siliceous mesoporous matrix enabled their application in acid and base catalysis[8–10]. The structure and properties of catalytically active centres in silicon-rich molecular sieves depend on the distribution of heteroatoms in the framework. Acidity of bridging OH groups can be affected by the presence of second Al atom in the zeolite ring and by the ring geometry[11,12]. Moreover, it is assumed that certain elementary steps in the reaction pathways may be favoured if two acid sites are close enough instead of being isolated[13]. Also stabilisation of divalent metal cations or metal–oxygen clusters, $[Me\text{-}O\text{-}Me]^{2+}$, is controlled by Al distribution. The activity of catalytic centres formed by extraframework divalent cations is affected by local co-ordination of these species and, thus, by distribution of Al pairs at different sites[14,15]. Recently it has been reported that a part of the framework Al atoms in (Al)MCM-41 is not located on its channel surface, but in the inner volume of the channel walls[3]. Therefore, in contrast to microporous zeolites, catalytic activity of (Al)MCM-41 cannot be directly related to the concentration of all aluminium atoms estimated from chemical analysis.

There are no available data (experimental or theoretical) on the Al distribution in mesoporous molecular sieves. ^{27}Al MAS NMR cannot provide any information on the location of Al atoms at the surface layer or inside the channel walls. ^{29}Si MAS NMR is able to distinguish only isolated Al atoms or Al-O-Si-O-Al sequences, but not Al-O-$(SiO)_2$-Al sequences, which represent a majority of close Al atoms in silicon-rich zeolites[16,17]. Moreover, in contrast to zeolites, there are no available data on the detailed local structure of the surface of mesoporous molecular sieve channels and this surface is usually regarded to be disordered/amorphous[18]. The surface is presented in simple models being formed from regular six-membered rings[19].

Recently, we have proposed Co^{2+} ions as a probe for the determination of Al pair distribution in silicon-rich molecular sieves[20–23]. This method is based on the determination of the ion exchange capacity of zeolite for the divalent cation under controlled conditions and on the quantitative evaluation of the spectra of "bare" Co^{2+} ions (without extraframework ligand) in different extraframework cationic sites. Only bare Co^{2+} ions balanced by two framework Al atoms in one ring are reflected in the d–d transitions (visible spectra) of dehydrated Co-containing zeolites. The number and distribution of bare Co^{2+} ions, characterise Al-O-$(SiO)_{1,2}$-Al sequences and their distribution in the alumosilicate framework. Moreover, the d–d transitions of bare Co^{2+} are a fingerprint of Co^{2+} ion co-ordination, *i.e.*, providing information on the geometry of cationic site.

In our recent paper[3] we have shown that Al distribution in (Al)MCM-41 is not controlled by statistical rules, but there is a different probability for location of Al atoms on the channel surface and inside the channel walls and the number of Al atoms on the channel surface depends on the framework Al content. This contribution is aimed at the understanding of the framework Al distribution in (Al)MCM-41 and of the effect of chemical composition and synthesis procedure on this distribution. In addition, an attempt is made to elucidate short-range ordering and local arrangement of the surface of the MCM-41 channel walls. The number of framework Al atoms on the surface of (Al)MCM-41 channels was characterised by the (Al)MCM-41 ion exchange capacity for Na^+ ions and pyridine adsorption followed by FTIR spectroscopy. The number of Al-O-$(SiO)_{1,2}$-Al sequences was determined from the exchange capacity for Co^{2+} ions. The distribution of Al pairs between different geometrical arrangements (cationic sites) was estimated using VIS spectroscopy of maximum exchanged dehydrated Co-(Al)MCM-41 molecular sieves. VIS spectroscopy was further applied to identify a local geometry arrangement of rings forming the surface of the MCM-41.

EXPERIMENTAL

(Al)MCM-41 Synthesis and Characterisation

Two different procedures were used for the synthesis of (Al)MCM-41. (Al)MCM-41/A (Si/Al = 11–140) was synthesised from sodium silicate (Riedel de Haen), hexadecyltrimethylammonium bromide (Fluka), ethyl acetate (Fluka) and aluminium hydroxide (Fluka); for details, see refs[13,24,25] (Al)MCM-41/B with Si/Al ratio from 13 to 112 was synthesised as follows. Initially, 2 g of hexadecyltrimethylammonium bromide (Fluka) was mixed with 240 g of distilled water and 21 ml of water solution of ammonium hydroxide (25%; Fluka) under stirring. Simultaneously, 20.1 g of tetraethyl orthosilicate (Fluka) was mixed with respective amount of aluminium isopropoxide (Fluka) and was slowly added to the first solution under vigorous stirring. The resulting mixture was aged at ambient temperature for 2 h. All samples were recovered by filtration, washed thoroughly with distilled water and dried at 350 K. To remove the structure-directing agent, the as-synthesised molecular sieves were calcined at 820 K for 6 h (temperature ramp = 1 K min^{-1}).

The structure of the synthesised, calcined and ion exchanged (Al)MCM-41 was checked using an X-ray powder diffractometer Siemens D5005 in the Bragg–Brentano geometry arrangement with CuKα radiation. XRD patterns evidenced a well-developed structure of MCM-41 (for details, see ref.[3]).

Adsorption isotherms of nitrogen were recorded at 77 K with an Accusorb 2100E instrument (Micromeritics). The samples were activated at 620 K and a pressure of 10^{-4} Pa for about 20 h.

^{27}Al MAS NMR spectra of (Al)MCM-41 samples were recorded by Dr P. Sarv (Estonia, Tallin) using hydrated forms of these molecular sieves and measured on a Bruker AMX500

spectrometer with a home-made probe heads with 3.5 mm o.d. rotors. The spinning speed was between 12 and 15 kHz and the r.f. strength about 70 kHz.

Ion Exchange of (Al)MCM-41

Na^+ and Co^{2+} ions were introduced into calcined (Al)MCM-41 *via* ion exchange at ambient temperature using sodium chloride and cobalt(II) nitrate solutions, respectively. To obtain maximum loading of Me-(Al)MCM-41 (Me = Na and Co), 1 g of (Al)MCM-41 was three times treated with 100 ml of 0.05 M $Co(NO_3)_2$ or 0.5 M NaCl for 24 h. Then, samples were carefully washed by distilled water, filtered and air-dried at ambient temperature. Chemical composition of calcined, Na- and Co-exchanged (Al)MCM-41, after their dissolution, obtained by atomic absorption spectrometry, is given in Table I. The number of (Al)MCM-41 sample in the table corresponds to its Si/Al composition.

UV-VIS-NIR Diffuse Reflectance Spectroscopy

UV-VIS-NIR diffuse reflectance (DR) spectra were recorded using a Perkin–Elmer UV-VIS-NIR spectrometer Lambda 19 equipped with a diffuse reflectance attachment with an integrating sphere coated with $BaSO_4$. The spectra were recorded in a differential mode with the corresponding Na-sample as a reference[20,21]. The absorption intensity was calculated from the Schuster–Kubelka–Munk equation $F(R_\infty) = (1 - R_\infty)^2/2R_\infty$, where R_∞ is the diffuse reflectance of a semi-infinite layer and $F(R_\infty)$ is proportional to the absorption coefficient.

Prior to the spectra monitoring, the Co-samples and parent Na-samples were dehydrated at 750 K and 7×10^{-2} Pa for 3 h. Dehydration was carried out with a heating rate of 5 K min^{-1}. After dehydration, the sample was cooled down to ambient temperature and transferred under vacuum into the optical cell and sealed.

FTIR Spectroscopy

The concentration of individual acid sites in (Al)MCM-41 was determined after adsorption of pyridine followed by FTIR spectroscopy using a Nicolet FTIR Protégé 460 spectrometer equipped with MCT detector and a cell with KBr windows connected to vacuum apparatus. (Al)MCM-41 samples were pressed into self-supporting wafers with a density of 7–12 mg cm^{-1}. Pyridine was degassed by repeated freezing and thawing cycles before its use. Prior to the ad-

TABLE I
Maximum Co, Na and Li loadings and pyridine adsorption in (Al)MCM-41 molecular sieves

Molecular sieve	Si/Al	Na/Al	Co/Al	Py/Al	Molecular sieve	Si/Al	Na/Al	Co/Al	Py/Al
(Al)MCM-41/A11	11	0.56	0.17	0.34	(Al)MCM-41/B13	13	0.45	0.16	0.41
(Al)MCM-41/A15	15	0.65	0.23	–	(Al)MCM-41/B28	28	0.5	0.22	0.53
(Al)MCM-41/A19	19	0.77	0.26	0.37	(Al)MCM-41/B46	46	0.78	0.27	0.56
(Al)MCM-41/A40	40	0.86	0.35	0.44	(Al)MCM-41/B60	60	1	0.45	–
(Al)MCM-41/A76	76	0.94	0.44	0.68	(Al)MCM-41/B112	112	1	0.45	0.82
(Al)MCM-41/A140	140	1.00	0.45	–					

sorption of pyridine, (Al)MCM-41 samples were activated in situ by overnight evacuation at 720 K. Pyridine was admitted to interact with active sites of (Al)MCM-41 at 420 K and partial pressure of 750 kPa for 30 min. The adsorption was followed by evacuation for 20 min. All measured spectra were recorded at room temperature with a resolution of 2 cm^{-1} by collecting 200 scans for a single spectrum and were recalculated to a normalised wafer density of 10 mg cm^{-1}. To determine the concentration of Lewis (ε_L) and Brønstedt (ε_B) acid sites, the following extinction coefficients were used: ε_L = 1.67 and ε_B = 2.22 cm μmol^{-1} (ref.[26]).

RESULTS

Characterisation of (Al)MCM-41

All synthesised and calcined (Al)MCM-41 molecular sieves exhibited well-ordered mesoporous structure possessing 4–5 well discernible diffraction lines in low-angle region of 2θ (not given here). In the case of adsorption isotherms of nitrogen, all samples exhibited a similar shape with a steep increase at the relative pressure $P/P_0 \approx 0.3$. This evidences the typical well-ordered structure of MCM-41 with the surface areas of mesopores in the range of 1000–1100 $m^2\ g^{-1}$ and their volumes 0.820–0.855 $cm^3\ g^{-5}$. The respective diameter of mesopores was about 3.4–3.5 nm. Thickness of walls was, according XRD and nitrogen adsorption, 1.2 nm for (Al)MCM-41/A and 0.85 nm for (Al)MCM-41/B. For details, see ref.[3]

Ion Exchange Capacity of (Al)MCM-41

Maximum loading of both Na and Co in both series (Al)MCM-41/A and B increases with the framework Al content (Table I). The maximum ion exchange capacity for both cations reaches almost 100% only at low framework Al contents (Si/Al > 100). With increasing content of Al in the framework the ion exchange capacity of both (Al)MCM-41/A and B for Na^+ and Co^{2+} ions significantly decrease.

UV-VIS-NIR Spectroscopy of Co-(Al)MCM-41

In UV-VIS spectra of hydrated Co-(Al)MCM-41, only asymmetric absorption band at 19 300 cm^{-1} was observed (not presented here). This band is characteristic of octahedral co-ordination of Co^{2+} ions in the hexaaqua complex balanced by two close framework Al atoms[15,16]. Continuous absorption from the NIR to UV region, characteristic of the formation of oxidic Co species, was not observed. Thus, only single Co^{2+} ions are present in investigated dehydrated Co-(Al)MCM-41. This finding is supported by exclusive

presence of the Co^{2+} hexaaqua complex in re-hydrated samples (not shown in figures).

In the case of dehydrated Co-(Al)MCM-41, the absence of the bands at 5260 and 7120 cm^{-1} (δ+ν and 2ν combination vibration bands of water molecule) in the NIR spectrum (not shown here) reflects dehydration of the molecular sieve. In addition, Co–OH groups were not formed during dehydration in Co-(Al)MCM-41. This evidences that only "bare" Co^{2+} ions, coordinated to framework oxygens are present in dehydrated samples.

The VIS spectra of dehydrated Co-(Al)MCM-41/A and B with different Si/Al ratios and maximum Co loading are shown in Fig. 1. The significant changes in the spectra indicate the presence of several spectral components. The second-derivative mode (not shown) and decomposition of the spectra to the Gaussian curves, illustrated in Fig. 2, were used to analyse the

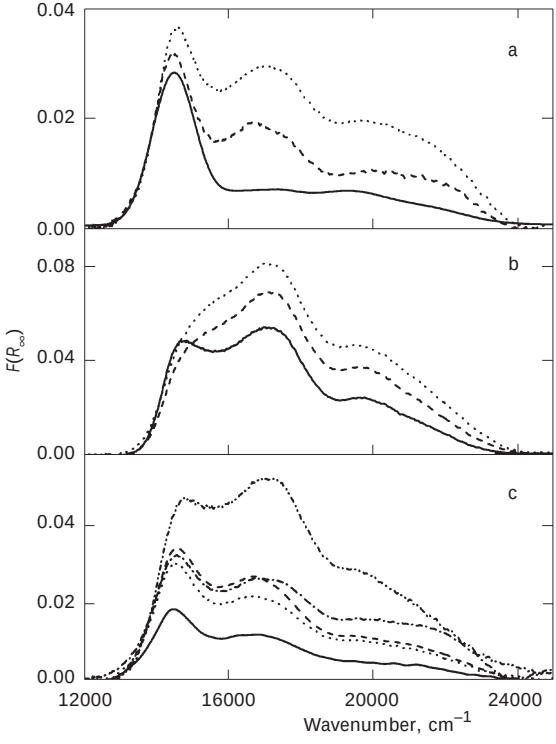

FIG. 1

VIS spectra of dehydrated Co-(Al)MCM-41/A140 (———), 76 (– – –) and 40 (· · · ·) (a); Co-(Al)MCM-41/A19 (———), 15 (– – –) and 11 (· · · ·) (b); Co-(Al)MCM-41/B112 (———), 60 (– – –), 46 (· · · ·), 28 (· – · – ·) and 13 (· · – · ·) (c)

spectra[20,21,27]. This enabled the assignment of absorption bands to two types of Co^{2+} ions, which indicates two types of cationic sites accommodating Co^{2+} (note that only "bare" Co^{2+} ions are present in dehydrated samples). Co-1 ions are reflected in the VIS spectrum by a single band with maximum at 14 600 cm^{-1}. Four bands at 15 850, 17 450, 19 970 and 21 700 cm^{-1} represent the Co-2 ions.

The decomposition of VIS spectra to Gaussian curves enabled estimation of absorption coefficients k_1 and k_2 corresponding to Co-1 and Co-2 ions and, thus, estimation of the concentration of these ions in molecular sieves[20,21]. The resulting absorption coefficients are $k_1 = 1.8 \times 10^{-3}$ and $k_2 = 3.7 \times 10^{-4}$ cm mmol g^{-1}. Co-1 ions prevail in (Al)MCM-41 with low-aluminium framework. Co-1 ions make about 65–80% of Co ions in Co-(Al)MCM-41 (Si/Al ≥ 100). Their relative population continuously decreases with increasing framework Al content to only 20–30% of Co ions in Co-(Al)MCM-41 at Si/Al ≤ 13.

FTIR Spectroscopy of (Al)MCM-41

FTIR spectra in the region of OH vibration of unloaded calcined (Al)MCM-41 consist only of a band at 3745 cm^{-1} corresponding to the terminal silanol groups. An additional band at 3660 cm^{-1} attributable to hydroxy groups on octahedrally co-ordinated Al atoms[28] was not observed. This confirms that no extraframework aluminium species are present in samples under study. No absorption band in the region 3600–3610 cm^{-1}

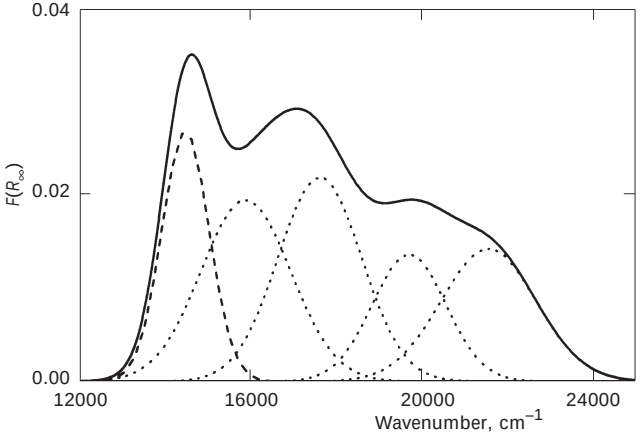

FIG. 2
Decomposition of the VIS spectrum of Co-(Al)MCM-41/A40 (———) into Gaussian curves corresponding to Co-1 (– – –) and Co-2 (· · · ·)

was observed, which means that no bridging acidic OH groups are present in the molecular sieves (Figs 3a and 4a). This is in contrast to data of Corma *et al.*[29], who found an absorption band at 3604 cm^{-1} after template removal in vacuum.

Pyridine adsorption was investigated in both series of (Al)MCM-41 to provide a quantitative analysis of the concentration of Brønsted and Lewis sites. Pyridine adsorption resulted in both series of (Al)MCM-41/A and B in the formation of a new band at about 1455 cm^{-1}, which corresponds to its coordinative interaction with electron acceptor sites (Lewis acid). The intensity of this band decreased with decreasing concentration of aluminium

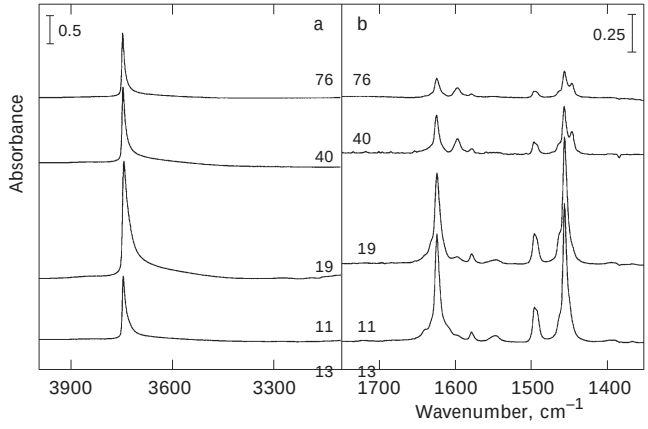

FIG. 3
Pyridine adsorption followed by IR spectroscopy in a series of (Al)MCM-41/A

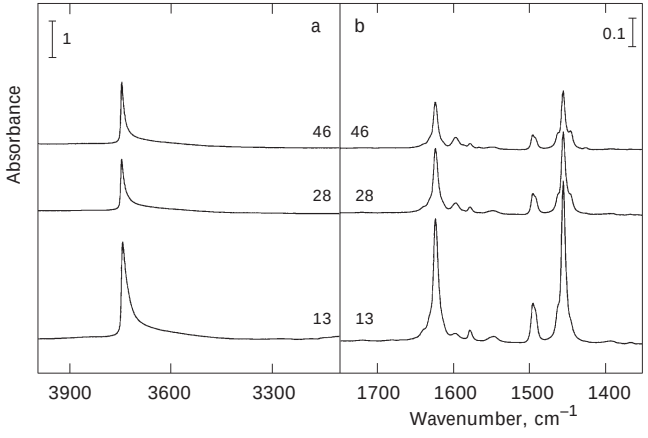

FIG. 4
Pyridine adsorption followed by IR spectroscopy in a series of (Al)MCM-41/B

in the samples (Figs 3b and 4b). In the case of samples (Al)MCM-41/A40 and A76, an additional band at 1445 cm^{-1} was observed in the spectrum (Fig. 3b), which could indicate the presence of two types of Lewis acid sites of different acidity[28]. Only negligible bands at 1545 cm^{-1} corresponding to pyridinium ion (PyH^+) were found in samples[24,30]. This evidences that practically no acidic OH groups are present in the samples. The maximum concentration of accessible aluminium atoms for (Al)MCM-41/A11 and (Al)MCM-41/B13 was found to be 0.43 and 0.48 mmol g^{-1}, respectively, which gives the maximum "surface" concentration of aluminium in the samples. The ratio of pyridine adsorbed related to "bulk" concentration of aluminium is given in Table I. This value increases with decreasing concentration of aluminium in (Al)MCM-41 and although the differences in the absolute amount of accessible Al atoms to pyridine and Na^+ were observed, both methods provided the same trend (Table I).

A characteristic ^{27}Al MAS NMR spectrum of sample (Al)MCM-41/A19 is depicted in Fig. 5. This spectrum evidences that in high-aluminium (Al)MCM-41 samples, the tetrahedrally co-ordinated aluminium dominates, its concentration being higher than 90%.

DISCUSSION

Location of Al Atoms on the Channel Surface and Inside the Channel Walls

Na^+ ions after ion exchange in aluminosilicate molecular sieves compensate the negative charge of the aluminosilicate framework and are located in the

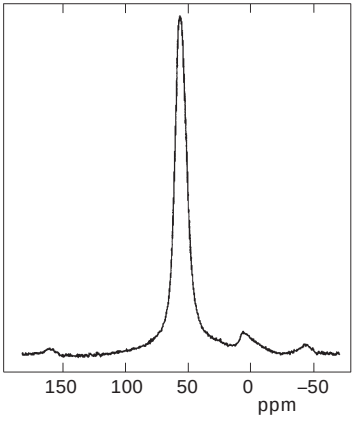

FIG. 5
Typical ^{27}Al MAS NMR spectrum of (Al)MCM-41/Al5

vicinity of Al atoms. In the case of (Al)MCM-41 with the walls formed from more than two layers of AlO_4 or SiO_4 tetrahedra, the Na^+ ions can be exchanged only in the vicinity of AlO_4 tetrahedra forming the surface layer of the channel walls. Thus, the maximum exchange capacity of molecular sieve for Na^+ ions reflects the number of framework Al atoms in the surface layer of the MCM-41 channel wall.

The significant decrease in the maximum of Na ion exchange capacity with increasing framework aluminium content (Table I) indicates that Al atoms are located not only in the surface layer of the (Al)MCM-41 channels, but also inside the channel walls. At low framework Al content, the surface Al atoms make 95–100% of Al atoms present in the (Al)MCM-41 while with increasing Al content only 45–55% of Al atoms are on the channel surface (Table I).

The results of Na^+ ion exchange and pyridine adsorption indicate that a significant part of Al atoms is incorporated inside the channel walls in (Al)MCM-41 with Si/Al lower than 20 (according to the chemical analysis). This causes a dramatic difference between the number and the density of surface Al atoms and thus, in the number of exchangeable sites according to bulk analysis of the sample and real values.

Number of Surface Al Atoms

The number of surface Al atoms can be characterised by the parameter Si/Al_{SURF}, defined as:

$$Si/Al_{SURF} = [Si]/[Al_{SURF}] \,, \qquad (1)$$

where [Si] is molar Si concentration according to bulk analysis, $[Al_{SURF}]$ molar concentration of surface Al atoms (reflected as exchanged Na^+ ions). Si/Al_{SURF} is easy to estimate using relation (*2*)

$$Si/Al_{SURF} = (Si/Al)/(Na_{MAX}/Al) \,, \qquad (2)$$

where Na_{MAX}/Al and Si/Al are the values obtained from bulk analysis of maximum Na-exchanged (Al)MCM-41. This number characterises the maximum concentration of accessible aluminium sites on the surface of walls in (Al)MCM-41. The effect of the framework Al content and synthetic procedure on the number of surface Al atoms in (Al)MCM-41 is depicted in

Fig. 6. For Si/Al ≥ 45, there is almost no difference between Si/Al and Si/Al_{SURF} values for both syntheses procedures of (Al)MCM-41/A and B. At high Al concentrations in the framework, only a part of Al atoms is incorporated into the surface of channel walls and Si/Al_{SURF} is significantly higher (*ca* twice for Si/Al ≤ 13) than bulk Si/Al. The minimum obtained Si/Al_{SURF} for (Al)MCM-41/B is lower than that of (Al)MCM-41/A. In general, the synthesis of (Al)MCM-41 with high framework Al content (Si/Al < 20) does not result in the preparation of molecular sieves with an adequately high number of surface Al atoms.

The discrepancy between chemical composition (Si/Al) and the number of surface Al atoms could explain the fact that no straightforward relationship between the conversion and chemical composition of (Al)MCM-41 was found, *e.g.*, for Knoevenagel condensation of benzaldehyde with malononitrile over Cs-exchanged (Al)MCM-41 [31], or for toluene alkylation with propylene over (Al)MCM-41 [22].

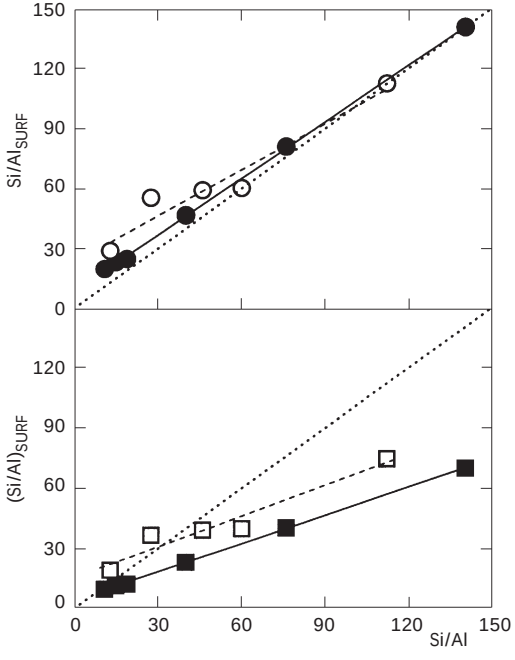

FIG. 6

Effect of chemical composition and synthetic procedure on the number of Al atoms on the surface of (Al)MCM-41 walls (Si/Al_{SURF}) (a): (Al)MCM-41/A (●), (Al)MCM-41/B (○) and density of Al atoms on the surface of (Al)MCM-41 walls ($(Si/Al)_{SURF}$) (b): (Al)MCM-41/A (■), (Al)MCM-41/B (□)

Density of Surface Al Atoms

In the case of zeolites, the density of Al atoms is given, similarly to the number of active sites, by the bulk analysis (Si/Al). For (Al)MCM-41, significant deviation between bulk Si/Al composition and Al density was described. $(Si/Al)_{SURF}$ (the surface Al density) depends on the location of both Al and Si atoms in the surface layer of channel walls. Thus, the number of layers forming the walls has to be taken into account. Because the dimensions of AlO_4 and SiO_4 tetrahedra are similar, the number of layers forming (Al)MCM-41 wall is given by the wall thickness. The arrangement of SiO_4 tetrahedra forming MCM-41 walls is not known, but the number of layers in the MCM-41 (N) can be roughly estimated according to the Eq. (*3*):

$$N = (T - 2D_O)/D_T \,, \qquad (3)$$

where N is an integer number, T is wall thickness estimated from X-ray diffraction and nitrogen adsorption isotherms, D_O is the distance between surface oxygen layers and corresponding layer of Si atoms (*ca* 0–0.04 nm), D_T corresponds to the distance between two layers of Si atoms (*ca* 0.30–0.32 nm). Values of D_O and D_T were taken from models of FER, MFI and BEA zeolites[32]. The number of surface Si atoms (Si_{SURF}) is given by Eq. (*4*):

$$Si_{SURF} = Si(2/N) \qquad (4)$$

and the surface Al density, $(Si/Al)_{SURF}$, is given by Eq. (*5*):

$$(Si/Al)_{SURF} = Si_{SURF}/Al_{SURF} = (Si(2/N))/(Na_{MAX}/Al) \,. \qquad (5)$$

The effect of framework Al content (expressed as Si/Al) and of the synthetic procedure on the surface Al density of (Al)MCM-41/A (wall thickness *ca* 1.2 nm, *i.e.* formed by 4 layers) and (Al)MCM-41/B (wall thickness *ca* 0.85 nm, *i.e.* formed by 3 layers) is also depicted in Fig. 6b. The surface Al density in (Al)MCM-41 is significantly higher (*ca* twice for Si/Al ≥ 100) than it should be on the basis of bulk analysis. With increasing Al content, this deviation decreases and for Si/Al ≤ 15 reaches values close to those based on bulk analysis.

The effect of the surface Al density, $(Si/Al)_{SURF}$, on the probability of the incorporation of Al atoms in the channel surface is shown in Fig. 7. The probability of incorporation corresponds to the ratio of the number of surface Al atoms (Al_{SURF}) to that of all Al atoms in (Al)MCM-41 framework. There is a significant preference to the incorporation of Al atoms in the surface layer of MCM-41 walls at low framework Al contents. The probability of the location of aluminium atoms in the surface layer (accessible sites) assuming to the random Al distribution is equal to 0.5 for (Al)MCM-41/A (4 layers in the wall) and 0.66 for (Al)MCM-41/B (3 layers). This preference sharply falls down at low $(Si/Al)_{SURF}$ indicating a limiting value for the density of Al atoms on the (Al)MCM-41 channel surface.

Distribution of Al Pairs and Single Al Atoms in the Channel Walls

Exclusive formation of "bare" Co^{2+} ions was observed after dehydration, thus the Co^{2+} ion exchange capacity is a measure of the number of (Al-O-$(SiO)_{1,2}$-Al) sequences in the surface layer of the (Al)MCM-41 channel walls. Because the possible presence of three Al atoms in the local structure formed by two rings in (Al)MCM-41 cannot be excluded (in contrast to silicon-rich zeolites), the number of (Al-O-$(SiO)_{1,2}$-Al) sequences present on the (Al)MCM-41 channel surface could be even higher than it follows from the ion exchange capacity. Similar ion exchange capacity of (Al)MCM-41 both for Co^{2+} and Na^{+} ions indicates that most of Al atoms on the

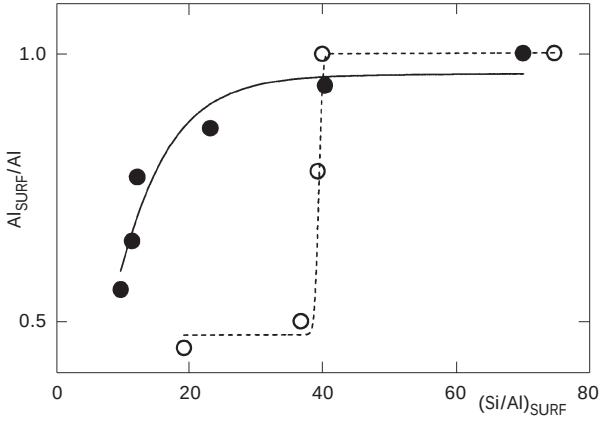

FIG. 7
Effect of chemical composition and synthesis procedure on the probability of the incorporation of Al atoms into surface layer (Al_{SURF}/Al) of the walls of (Al)MCM-41/A (●) and (Al)MCM-41/B (○)

(Al)MCM-41 channel surface (60–90%) correspond to close Al atoms forming Al-O-$(SiO)_{1,2}$-Al sequences.

The effect of the framework Al content in (Al)MCM-41/A and B on the relative concentration of Al-O-$(SiO)_{1,2}$-Al sequences is shown in Fig. 8. The Al-O-$(SiO)_{1,2}$-Al sequences prevail in the whole range of Al contents of (Al)MCM-41 independently of the synthetic procedure. At low framework aluminium contents, Al-O-$(SiO)_{1,2}$-Al sequences contain 95% of Al atoms. With increasing Al content, the number of Al-O-$(SiO)_{1,2}$-Al sequences decreases and for Si/Al = 13, Al-O-$(SiO)_{1,2}$-Al sequences contain 60% of Al atoms. There are no substantial differences between the above described dependence of Al distribution on Si/Al and its dependence on Si/Al_{SURF} or $(Si/Al)_{SURF}$. The predominant formation of Al-O-$(SiO)_{1,2}$-Al sequences at low framework Al contents is in contradiction with the prediction based on the random distribution of Al atoms in aluminosilicate molecular sieves. It indicates that the Al distribution in (Al)MCM-41 is not controlled by statistic rules, which is in agreement with Al distribution in ZSM-5 [18,19]. However, in contrast to ZSM-5, a particular effect of synthesis procedure on the formation of Al-O-$(SiO)_{1,2}$-Al sequences was not observed. The total number both of single Al atoms and Al-O-$(SiO)_{1,2}$-Al sequences in (Al)MCM-41 increases with increasing Al content in the framework, but at lowest values of Si/Al ratio, the number of single Al atoms increases significantly faster than the number of Al-O-$(SiO)_{1,2}$-Al sequences.

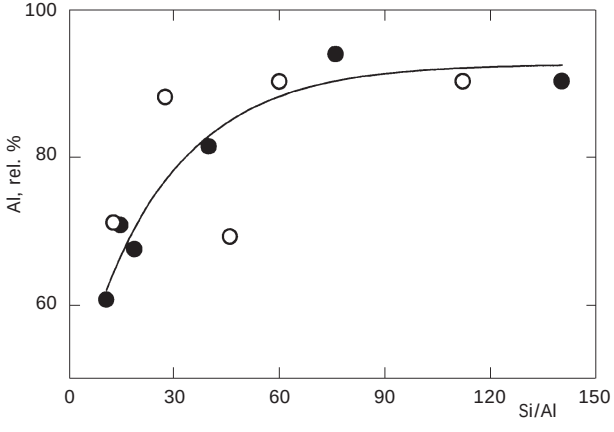

FIG. 8
Effect of chemical composition and synthetic procedure on the relative concentration of Al atoms in surface Al-O-$(SiO)_{1,2}$-Al sequences in (Al)MCM-41/A (●) and (Al)MCM-41/B (○)

Distribution of Al-O-$(SiO)_{1,2}$-Al Sequences on the Channel Surface

As follows from the spectra of Co-(Al)MCM-41 with different Co loadings and the decomposition of the spectra into the Gaussian curves (see Figs 1 and 2) as well as from the exclusive presence of "bare" Co^{2+} ions, the Al-O-$(SiO)_{1,2}$-Al sequences are present on the (Al)MCM-41 channel surface in two different local geometries, reflected in the formation of Co^{2+} ions of the type Co-1 and Co-2. Concentration of the Co-1 and Co-2 ions, estimated using Eq. (*1*) and absorption coefficients k_1 and k_2 (see Results) in maximum Co-loaded Co-(Al)MCM-41 is a measure of the concentration of Al-O-$(SiO)_{1,2}$-Al sequences (one sequence corresponds to one Co^{2+} ion) at individual cationic sites. The effect of the framework Al content on the concentration of Al atoms in cationic sites accommodating Co-1 and Co-2 ions in maximum-loaded Co-(Al)MCM-41 is depicted in Fig. 9. The Al-O-$(SiO)_{1,2}$-Al sequences forming the cationic site for Co-1 ions are formed preferentially at the lowest Al content in (Al)MCM 41 and the number of possible framework arrangements accommodating these pairs is limited. With increasing incorporation of Al atoms into the framework, Al-O-$(SiO)_{1,2}$-Al sequences accommodating Co-2 ions are preferentially formed. The preferential formation of one type of Al-O-$(SiO)_{1,2}$-Al sequences was reported also for ZSM-5, depending on the synthetic procedure[18,19]. The concentration of Al-O-$(SiO)_{1,2}$-Al sequences of type Co-2 is about twice higher for (Al)MCM-41/A compared to (Al)MCM-41/B.

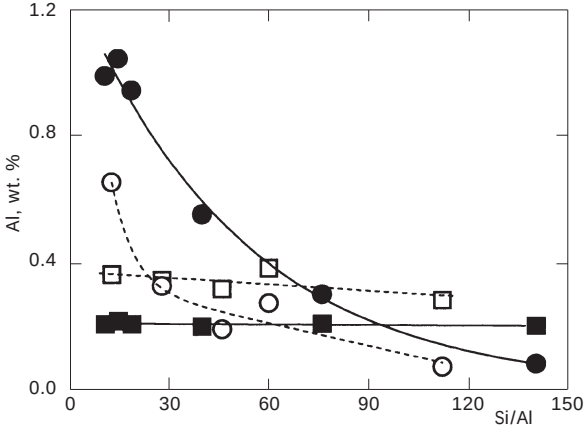

FIG. 9
Effect of chemical composition and synthetic procedure on the concentration of Al atoms in Al-O-$(SiO)_{1,2}$-Al sequences at Co-1 site, (Al)MCM-41/A (■), (Al)MCM-41/B (□) and at Co-2 site (Al)MCM-41/A (●), (Al)MCM-41/B (○)

Uniformity of Cationic Sites

The co-ordination of the Co^{2+} ion to the cationic site is followed by deformation of the site geometry. However, despite this rearrangement of the geometry of cationic sites, the spectra of Co^{2+} ions reflect small differences in the geometry of similar sites in different zeolites. Thus, even small differences in the local arrangement of cationic sites and/or their environment are reflected in the spectrum of bare Co^{2+} ions. Also different Al distribution in the cationic site (Al-O-Si-O-Al and Al-O-$(SiO)_2$-Al sequences of different framework T sites occupied by Al atoms in zeolites) is followed by substantial differences in the local geometry of co-ordination of divalent cation in the same local geometry of the framework, as follows from computing studies[33–36]. Only bands corresponding to Co-1 and Co-2 ions were observed in(Al)MCM-41 of a wide range of Si/Al/Co chemical composition and the band widths are similar to those reported for Co-zeolites (Table II). This indicates that Co-1 and Co-2 cationic sites are two uniform types of local framework arrangement (in the sense of uniformity of individual types of cationic sites in zeolite) with uniform Al distribution.

Geometry of Cationic Sites

The d–d transitions of the Co^{2+} ions reflected in the VIS spectrum are sensitive to the local environment of the ion. Thus, VIS spectra of bare Co^{2+} ions can been used as fingerprints of the geometry of the cationic sites in molecular sieves (for details, see refs[20,21]). As follows from Table II, the VIS spectra of Co-1 and Co-2 ions are similar to those of Co^{2+} ions in MOR, FER and MFI zeolites[20,21,37]. The spectrum of Co-1 ions is similar to that of Co^{2+} ions

TABLE II
Spectra of bare Co(II) ions in Co-(Al)MCM-41 (Co-1,2) and in pentasil-ring zeolites (Co-α,β,γ)

Matrix	Co(II) bands, cm^{-1}							Band width, cm^{-1}		
	Co-1/α		Co-2/β			γ		Co-1/α	Co-2/β	γ
MCM-41	14 500	15 500	17 300	19 700	21 500			1200	2200	
MOR	14 800	15 900	17 500	19 200	21 100	20 150	22 050	1200	2100	1300
FER	15 000	16 000	17 100	18 700	20 600	20 300	22 000	1100	1900	1200
ZSM-5	15 100	16 000	17 150	18 600	21 200	20 100	22 000	1800	2100	1400

of the α-type. These Co^{2+} ions are co-ordinated on the top of the pyramid of four framework oxygens of the elongated six-membered ring formed by two connected five-membered rings in pentasil-ring zeolites. Local arrangement of this cationic site in pentasil-ring zeolites is schematically depicted in Fig. 10a.

The spectrum of Co-2 ions is similar to the spectra of Co^{2+} ions of the β-type. These Co^{2+} ions exhibit approximately planar co-ordination in the plane of the deformed ring of six framework oxygen atoms. Local arrangements of these cationic sites in pentasil-ring zeolites are schematically depicted in Fig. 10b–10d. Note that six oxygen atoms of twisted eight-membered ring of mordenite are located approximately in plane, two remaining oxygen atoms of this ring are far from the ring centre and their effect on the Co^{2+} ligand field can be neglected.

Spectra similar to those of Co-1 and Co-2 ions were never observed with other than the above listed pentasil ring structures (*cf.* refs[38–43]). Location of the Co^{2+} ion in the single regular six-membered ring of the A zeolite structure is characterised by a significant doublet around 25 000 cm^{-1} (ref.[36]). Co^{2+} ions located in the regular six-membered ring of the faujasite hexagonal prism are characterised by two bands between 13 500 and 16 000 cm^{-1} (trigonal Co^{2+} co-ordination) or by a triplet with maxima position between 15 000 and 19 550 cm^{-1} (pseudo-tetrahedral co-ordination). Co^{2+} ions located inside the faujasite hexagonal prism exhibit absorption bands between 17 850 and 20 000 cm^{-1} (pseudo-octahedral co-ordination)[39–41].

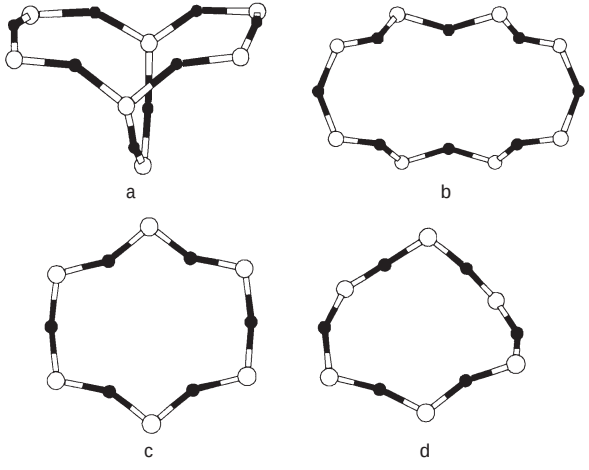

FIG. 10
Local arrangement of Co-α site in ferrierite (a) and Co-β site in mordenite (b), ferrierite (c), ZSM-5 (d); Al and Si atoms (○), oxygen atoms (●)

Thus, the Co-1 type of cationic site can be suggested to represent elongated six-membered ring composed of two five-membered rings. The Co-2 type of cationic site represents a deformed six-membered ring of framework oxygens. Because the presence of a significant number of twisted eight-member rings on the surface of (Al)MCM-41 channels is of low probability, two types of deformed six-membered rings (single planar and composed of two five-membered rings) containing two framework Al atoms and accommodating bare divalent cations can be proposed to be located on the (Al)MCM-41 inner surface.

Uniformity/Ordering of the Surface of the MCM-41 Channels

It can be hardly assumed that the uniformity of the cationic site from the point of view of its geometry, deformation properties and its environment should be achieved for the site rings with different environment (neighbouring rings) in the flexible framework of molecular sieve. Thus, the uniformity of larger area (greater number of the surface silicon/aluminium framework atoms) is necessary to guarantee the uniformity of the local arrangement of Co^{2+} cationic sites. The nearest neighbours of the atoms forming deformed six-membered rings (minimum size of ring accommodating cation in pentasil ring zeolites) at least and their next-nearest neighbours (with high probability) should be arranged uniformly. This indicates that two types of uniform domains are present on the surface of the (Al)MCM-41 channels. Deformed planar or bent six-membered rings are located in their centres. These surface domains are composed of more than 18 surface silicon/aluminium atoms in the case of central ring surrounded by five-membered rings and from more than 24 surface silicon/aluminium atoms in the case of central ring surrounded by six-membered rings.

The number of surface silicon/aluminium atoms belonging to the regular domains can be also estimated. The highest Co loading was achieved with Co-(Al)MCM-41/A possessing Si/Al = 15. For this sample, the surface Al density ($(Si/Al)_{SURF}$) was 11 and the corresponding Co/Al_{SURF} ratio reached 0.35. From this density of the bare Co ions on the (Al)MCM-41 channel surface it follows that 31 surface silicon/aluminium atoms correspond to one Co^{2+} ion. Thus, 60–80% of the surface atoms belong to uniform domains of nearest and next-nearest neighbours. Note that these numbers were obtained for the minimum possible size of regular domain and thus, are the lowest limits of atoms located in the regular domains on the channel surface. It can be concluded that uniform domains form a dominant part of the surface of (Al) MCM-41 channel walls.

Parameters Controlling Al Distribution in (Al)MCM-41 During Synthesis

The Al distribution on/in the channel walls, formation of single Al atoms and Al-O-$(SiO)_{1,2}$-Al sequences and distribution of Al-O-$(SiO)_{1,2}$-Al sequences at different cationic sites are not controlled by statistic rules. In a similar way to ZSM-5 [19], it is possible to infer that the synthetic procedure plays the key role controlling the distribution of aluminium in individual zeolites or mesoporous molecular sieves.

The significant preference to the incorporation of Al atoms into the surface layer of the (Al)MCM-41 channel wall should be explained by electrostatic interaction. Anions containing Al atoms exhibit a higher charge compared to those containing only Si atoms. Thus, it can be assumed that they are preferentially driven to be located in the first layer interacting with cationic surfactant at the early stages of the synthesis. With increasing concentration of anions containing Al atoms in the first layer surrounding the surfactant, saturation of the surfactant charge by Al-containing species together with repulsion between them takes place. This results in a decrease in the probability of the location of Al-containing anions on the surface of surfactant micelles. $(Si/Al)_{SURF}$ *ca* 10 seems to be the limit concentration of Al atoms in the first layer surrounding the surfactant during synthesis. However, a different surface Al density $(Si/Al)_{SURF}$ achieved for (Al)MCM-41/A and B synthesised under different synthesis conditions indicates that synthesis temperature is only one of the parameters controlling the distribution of aluminium in (Al)MCM-41.

The preferential formation of Al-O-$(SiO)_{1,2}$-Al sequences in the whole Al concentration range, especially at low Al framework concentration indicates that the formation of Al-O-$(SiO)_{1,2}$-Al sequences proceeds at early stages of the synthesis followed by formation of large complex anions containing two Al atoms. Further confirmation of this hypothesis is required.

CONCLUSIONS

The distribution of Al atoms between the surface layer and inner layers of the channel walls of (Al)MCM-41 and the distribution of Al atoms between single Al atoms and Al-O-$(SiO)_{1,2}$-Al sequences depends on the framework Al content and conditions of the synthesis.

At low framework Al contents, Al atoms are located almost exclusively in the channel surface independently of the conditions of synthesis. With increasing framework aluminium content, Al atoms are incorporated also inside the channel walls. For (Al)MCM-41 with high Al contents ($Si/Al \leq 13$),

only 55% (synthesis A) and 45% (synthesis B) of Al atoms are placed on the molecular sieve inner surface and form cationic sites.

The Al-O-$(SiO)_{1,2}$-Al sequences dominate at low framework Al contents and are the prevailing form of framework aluminium atoms also on the channel surface of all (Al)MCM-41 with high framework Al contents. The formation of single Al atoms ($(SiO)_3$-Al-O-$(SiO)_{1,2}$) occurs only at high framework Al contents.

Two types of rings containing Al-O-$(SiO)_{1,2}$-Al sequences are proposed on the (Al)MCM-41 surface. The number of elongated six-membered rings composed of two five-membered rings containing two Al atoms does not change with the Al content in molecular sieve while the number of planar six-membered rings significantly increases with increasing content of framework aluminium in (Al)MCM-41. The arrangement of Al-O-$(SiO)_{1,2}$-Al sequences in these two local framework arrangements is uniform.

A majority (*ca* 80%) of the surface of the (Al)MCM-41 channels consists of two types of domains containing in their centres deformed bent or planar six-membered rings. These domains containing *ca* 24 surface silicon/aluminium atoms are uniform. The domains containing planar six-membered rings make a majority of ordered (Al)MCM-41 channel surface.

Financial support of the Grant Agency of the Academy of Sciences of the Czech Republic (A4040001 and S4040017), Grant Agency of the Czech Republic (104/02/0571) and Volkswagen Stiftung (I/75886) is highly acknowledged. The work of J. Kotrla was supported by a postdoctoral grant from the Grant Agency of the Czech Republic (203/00/8033). The authors thank Dr A. Zukal for adsorption isotherms of nitrogen, Dr P. Sarv (Tallin, Estonia) for recording ^{27}Al MAS NMR spectra and Dr T. Grygar for chemical analysis of molecular sieves.

REFERENCES AND NOTES

1. *International Symposium on Nanoporous Materials II, Banff 2000* (A. Sayari, M. Jaroniec, T. J. Pinnavaia, Eds), Elsevier; *Stud. Surf. Sci. Catal.* **2000**, *129*.
2. *International Symposium on Nanoporous Materials III, Ottawa 2002* (A. Sayari, M. Jaroniec, Eds), Elsevier; *Stud. Surf. Sci. Catal.* **2002**, *141*.
3. Dědeček J., Žilková N., Čejka J.: *Microporous Mesoporous Mater.* **2001**, *44–45*, 259.
4. Kresge C. T., Leonowicz M. E., Roth W. J., Vartuli J. C., Beck J. S.: *Nature* **1992**, *359*, 710.
5. Kooyman P. J., Slabová M., Bosáček V., Čejka J., Rathouský J., Zukal A.: *Collect. Czech. Chem. Commun.* **2001**, *66*, 555.
6. Dědeček J., Žilková N., Čejka J.: *Collect. Czech. Chem. Commun.* **2001**, *66*, 567.
7. Čejka J., Žilková N., Rathouský J., Zukal A.: *Phys. Chem. Chem. Phys.* **2001**, *3*, 5076.
8. Vartuli J. C., Shih S. S., Kresge C. T., Beck J. S.: *Stud. Surf. Sci. Catal.* **1998**, *117*, 13.
9. van Bekkum H., Kloestra K. R.: *Stud. Surf. Sci. Catal.* **1998**, *117*, 171.
10. Corma A., Kumar D.: *Stud. Surf. Sci. Catal.* **1998**, *117*, 201.

11. Gonzales N. O., Chakkraborty A. K., Bell A. T.: *Catal. Lett.* **1998**, *50*, 135.
12. Sauer J., Ugliengo P., Garrone E., Saunders V. R.: *Chem. Rev. (Washington, D. C.)* **1994**, *94*, 2095.
13. Schantz D. F., Fild Ch., Koller H., Lobo R.: *J. Phys. Chem. B* **1999**, *103*, 10858.
14. Kaucký D., Vondrová A., Dědeček J., Wichterlová B.: *J. Catal.* **2000**, *194*, 318.
15. Wichterlová B., Dědeček J., Sobalík Z.: *Catalysis by Unique Metal Ion Structures in Solid Matrices. From Science to Application, NATO Advanced Research Workshop, Prague-Průhonice, 2000* (G. Centi, B. Wichterlová and A. T. Bell, Eds), p. 31. Kluwer Academic Publishers, Dordrecht 2001.
16. Gobbi G. C., Kennedy G. J., Fyfe C. A.: *Chem. Lett.* **1983**, 1551.
17. Rice M. J., Chakraborty A. K., Bell A. T.: *J. Catal.* **1999**, *186*, 222.
18. Chen C.-Y., Li H.-X., Davis M. A.: *Microporous Mater.* **1993**, *2*, 17.
19. Gusev V.: http://boba.boom.ru/eng/msm-41.html (1998).
20. Dědeček J., Kaucký D., Wichterlová B.: *Chem. Commun.* **2001**, *11*, 970.
21. Dědeček J., Kaucký D., Gonsiorová O., Wichterlová B.: *Phys. Chem. Chem. Phys.* **2002**, *4*, 5406.
22. Dědeček J., Kaucký D., Wichterlová B.: *Microporous Mesoporous Mater.* **2000**, *35–36*, 483.
23. Dědeček J., Wichterlová B.: *J. Phys. Chem. B* **1999**, *103*, 1462.
24. Čejka J., Krejčí A., Žilková N., Dědeček J., Hanika J.: *Microporous Mesoporous Mater.* **2001**, *44–45*, 499.
25. Schulz-Ekloff G., Rathouský J., Zukal A.: *J. Inorg. Mater.* **1999**, *1*, 97.
26. Emeis C. A.: *J. Catal.* **1993**, *141*, 347.
27. Dědeček J., Žilková N., Čejka J.: *Stud. Surf. Sci. Catal.* **2000**, *129*, 235.
28. Jentys A., Phan N. H., Vinek H.: *J. Chem. Soc., Faraday Trans.* **1996**, *93*, 3287.
29. Corma A., Fornes V., Navarro M. T., Perez-Pariente J.: *J. Catal.* **1994**, *148*, 569.
30. Lercher J. A., Gruendling C., Eder-Mirth G.: *Catal. Today* **1996**, *27*, 353.
31. Ernst S., Bongers T., Casel C., Munsen S.: *Stud. Surf. Sci. Catal.* **1999**, *125*, 367.
32. www.iza-structure.org/databases.
33. Šponer J. E.: Private communication.
34. Nachtigallová D., Nachtigall P., Sierka M., Sauer J.: *Phys. Chem. Chem. Phys.* **1999**, *1*, 2019.
35. Nachtigallová D., Nachtigall P., Sauer J.: *Phys. Chem. Chem. Phys.* **2001**, *3*, 1552.
36. Nachtigall P., Davidová M., Nachtigallová D.: *J. Phys. Chem. B* **2001**, *105*, 3510.
37. Kaucký D., Dědeček J., Wichterlová B.: *Microporous Mesoporous Mater.* **1999**, *31*, 75.
38. Klier K.: *Adv. Chem. Ser.* **1971**, *101*, 480.
39. Klier K., Kellerman R., Hutta J. P.: *J. Chem. Phys.* **1974**, *61*, 4224.
40. Kellerman R., Klier K.: *Proc. Chem. Soc. London* **1975**, *4*, 1.
41. Verbeckmoes A. A., Weckhuysen B. M., Pelgrims J., Schoonheydt R. A.: *J. Phys. Chem.* **1995**, *99*, 15222.
42. Verbeckmoes A. A., Weckhuysen B. M., Schoonheydt R. A.: *Stud. Surf. Sci. Catal.* **1997**, *105*, 623.
43. Verbeckmoes A. A., Weckhuysen B. M., Pelgrims J., Schoonheydt R. A.: *Microporous Mesoporous Mater.* **1998**, *22*, 165.